Available online at www.sciencedirect.com
SCIENCE DIRECT®
Journal of Geodynamics 38 (2004) 93–115
JOURNAL OF GEODYNAMICS
http://www.elsevier.com/locate/jog

New paleomagnetic data from the northern Puna and western Cordillera Oriental, Argentina: a new insight on the timing of rotational deformation

Claudia Prezzi [a,*], Pablo J. Caffe [b], Rubén Somoza [c]

[a] *CONICET – Universidad de Buenos Aires – Research Fellow of the Alexander von Humboldt Foundation, Institut für Geowissenschaften, Abteilung Geophysik, Christian Albrechts Universität, Otto Hahn Platz 1, 24118 Kiel, Germany*
[b] *CONICET – Instituto de Geología y Minería, Universidad Nacional de Jujuy, Avda, Bolivia 1661, S. S. de Jujuy, Argentina*
[c] *CONICET – Instituto de Geofísica D. Valencio, Dpto. de Cs. Geológicas, FCEyN, Universidad de Buenos Aires, Ciudad Universitaria, Pabellón 2, 1428 Buenos Aires, Argentina*

Received 3 November 2003; received in revised form 26 April 2004; accepted 3 May 2004

Abstract

Along the Central Andes a pattern of vertical axis tectonic rotations has been paleomagnetically identified. The rotations are clockwise in southern Bolivia, northern Chile and northwestern Argentina. Various models have been proposed to explain the geodynamic evolution of the Central Andes, but the driving mechanism of these rotations remains controversial. Constraining the spatial variability and the timing of the rotations may contribute to a better understanding of their origin. Our results complement information from previous studies, improving the knowledge of tectonic rotations in the region of the northern Argentine Puna and western Cordillera Oriental. In the San Juan de Oro basin (SJOB), 132 cores were drilled from the middle Miocene Tiomayo Formation in the zone of Tiomayo–Santa Ana (22°30′S–66°30′W), and from the ∼17 Ma Casa Colorada dacite dome complex. Another 114 cores were collected from middle Miocene dacitic dome centers emplaced in the zone of Laguna de Pozuelos basin (22°30′S–66°00′W). The results of our paleomagnetic study suggest that the sampled zones underwent very low, statistically insignificant rotation since middle Miocene. However, a tendency for low magnitude rotation appears when observing our data together with paleomagnetic results from coeval rocks in neighbouring areas. If so, this low rotation could be related to middle Miocene thrust activity in the central and eastern parts of the Cordillera Oriental. The combined analysis of paleomagnetic and structural data illustrates the probable, direct relationship between timing of significant rotations and timing of local deformation in the sourthern Central Andes.

* Corresponding author. Fax: +54 11 47883439.
E-mail addresses: pabcaffe@gl.fcen.uba.ar (C. Prezzi), pabcaffe@idgym.unju.edu.ar (P.J. Caffe), somoza@gl.fcen.uba.ar (R. Somoza).

0264-3707/$ – see front matter © 2004 Elsevier Ltd. All rights reserved.
doi:10.1016/j.jog.2004.05.001

1. Introduction

Both the structural and topographic trends in the Central Andes encompass the curved shape of the western margin of South America. During a long time the origin of this morphostructural feature was attributed to oroclinal bending, the so-called Bolivian Orocline of Carey (1958). Later on a plausible oroclinal model was presented by Isacks (1988), who suggested that an ancient curvature of the margin was enhanced to accommodate along strike gradient of Neogene horizontal-shortening in the eastern part of the Central Andes. In its simplest expression, the oroclinal model predicts regional counterclockwise rotations in the northern branch of the orogen (Perú and northern Bolivia) and clockwise rotations in the southern branch (northern Chile, southern Bolivia, and northwestern Argentina). Paleomagnetically detected rotations show an overall consistency with this prediction (see compilations in Somoza et al., 1996; Randall, 1998; Beck, 1998; Prezzi and Alonso, 2002). However, the growing paleomagnetic database is showing a more complicated pattern, as dictated by variations in magnitude and timing of rotations (Somoza et al., 1996; Roperch et al., 2000; Somoza and Tomlinson, 2002; Rousse et al., 2003).

This paper focused on paleomagnetism from middle Miocene rocks in an area of the southern branch of the Central Andean salient. The studied rocks are particularly pertinent because they unconformably underlie unrotated upper Miocene ignimbrites. The aim of this study was further exploring the timing of rotations in this part of the orogen. Our new results suggest that any middle Miocene rotation in the study area was of very low magnitude, close to the resolution threshold of paleomagnetism. However, when observed together with available data from Neogene rocks in neighbouring areas, the group suggests the possibility of a pre-late Miocene, low magnitude rotation in the Puna/Altiplano and western border of the Cordillera Oriental at the latitude of the Bolivia/Argentina boundary.

2. Geologic setting

2.1. San Juan de Oro basin

Most Neogene sedimentary sequences in the northern Puna and southern Bolivian Altiplano (22°–24°S) are very similar and show a comparable Cenozoic stratigraphic record. The San Juan de Oro basin (SJOB) is the broadest Neogene basin in northern Puna (Figs. 1 and 2A), covering a large area whose basement—as with almost all the other basins in the area—is represented by Ordovician rocks, thin Cretaceous to Paleocene rocks (Salta Group) and Eocene to lower Miocene thick fluviatile redbed deposits (Peña Colorada Formation, Bellman and Chomnales, 1960). One of the main characteristics of early Neogene Puna basins shared by the SJOB, is the intercalation of sediments with volcanic products (Coira et al., 1993; Caffe and Coira, 2002). Since the upper Miocene, the infilling has been even more volcanic, almost exclusively composed of ignimbritic successions erupted from large caldera structures (de Silva, 1989; Coira et al., 1993, Fig. 2A).

2.1.1. Tiomayo Formation

Middle Miocene Tiomayo Formation (Seggiaro and Aniel, 1989) represents the typical infilling of local basins mentioned, and crops out across the southern half (∼2500 km^2) of the SJOB (Caffe and Coira, 2002). This sequence is a thinning- and fining-upward succession, which changes from red conglomerates and sandstones at the base to mostly yellow and greenish mudstones at the top, predominating the latter aspect in direction to the depocentre (Tiomayo; Fig. 2A).

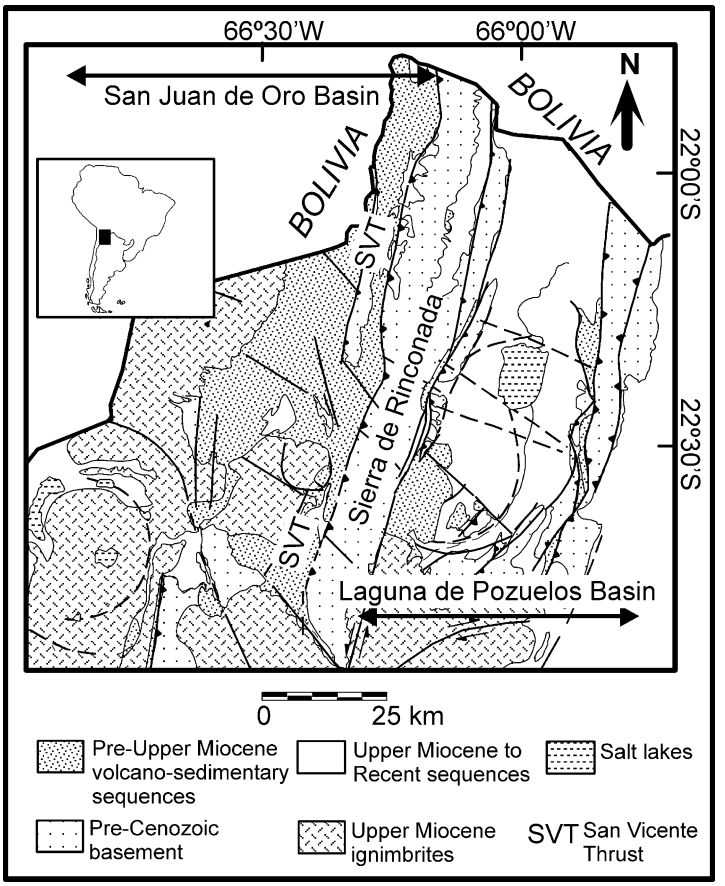

Fig. 1. Geologic map of northern Puna major sedimentary basins.

In the northeastern border of SJOB, the basal part of the Tiomayo Formation lies uncomformably over older units (pre-18 Ma Peña Colorada Formation, ~17 Ma Casa Colorada dacitic dome; Coira et al., in press; Caffe and Coira, 2002). Southward, the basal member of Tiomayo Formation onlaps directly over Ordovician basement rocks, either at the eastern (Sierra de Rinconada) or western margins (Mina Pirquitas) of the basin. In the basinal axis (Tiomayo–Santa Ana; Fig. 2A) the reddish section is however difficult to characterize, because the reddish member discomformably overlies the underlying Peña Colorada Formation. In this place, the transition between both units is vague. Thus, the passage from one to the other was redefined in terms of the presence of volcanic and evaporitic material: while in the Tiomayo Formation gypsum and halite are absent and the intercalation of pyroclastic beds is very common, the opposite comes about for the Peña Colorada Formation (Coira et al., in press).

In the Tiomayo–Santa Ana zone (Locality "A" in Fig. 2A), as well as in Mina Pirquitas area (Locality "B" in Fig. 2A), the reddish section involves a 40 m thick succession of fluviatile conglomerates, sandstones and mudstones that often are interbedded with pyroclastic flow deposits and air-fall tuffs. One ignimbrite from the base in the northern outcrops (Casa Colorada area) has been dated in 15.7 ± 0.6 Ma,

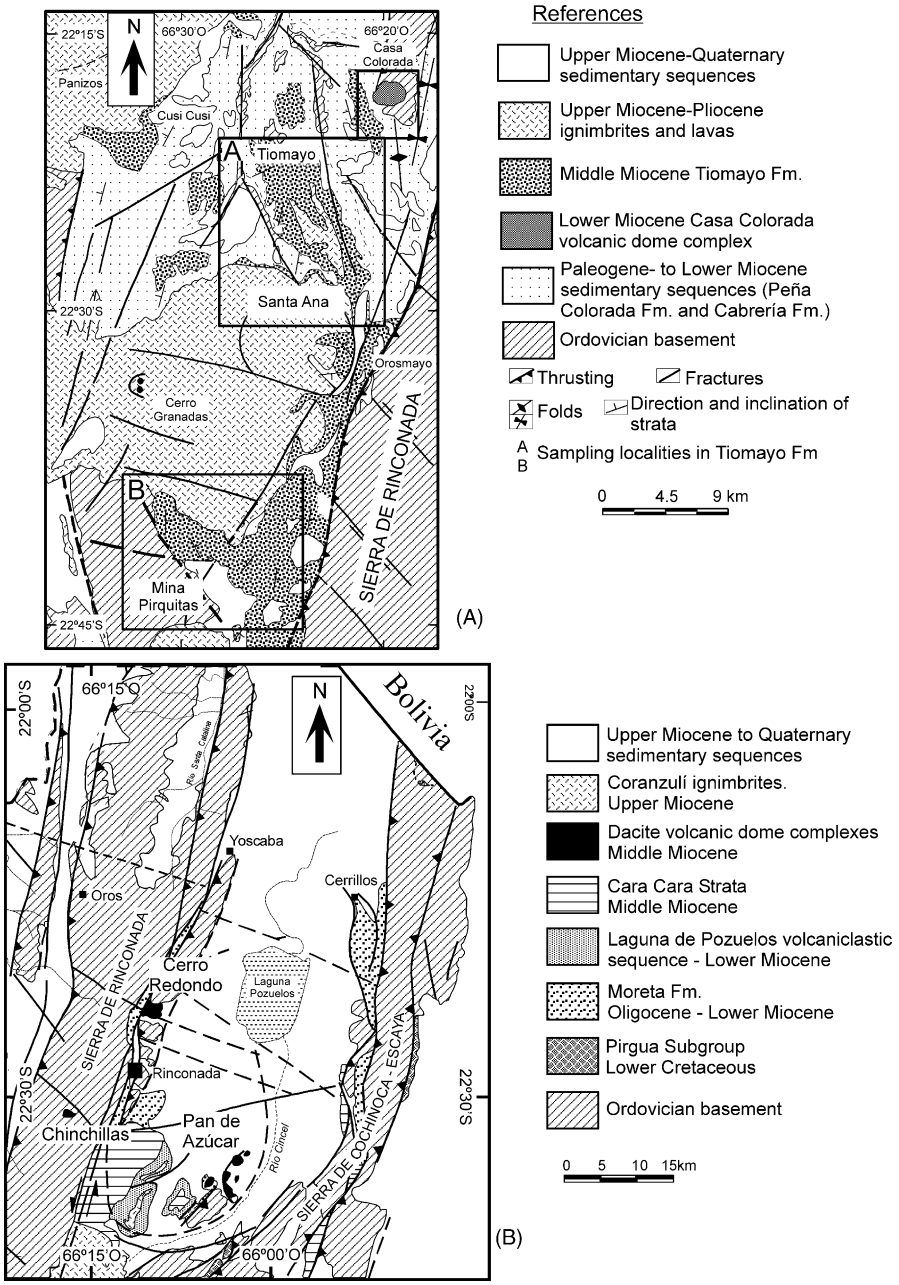

Fig. 2. (A) Geologic map of main Cenozoic units in the San Juan de Oro basin. (B) Geologic map of the Laguna de Pozuelos basin.

similar to a K–Ar age of 14.9 ± 0.5 Ma (Caffe and Coira, 2002) yielded by an ignimbrite in an equivalent position to the south (Mina Pirquitas).

The middle and upper sections of the Tiomayo Formation do not crop out south of Orosmayo (Fig. 2A), being well represented only in Santa Ana–Tiomayo zone. The middle section consists of a 50 m thick

yellowish succession of sandstones and mudstones, often intercalated with reworked tuffs in the upper half of the section.

The upper member of the Tiomayo Formation (70 m thick) is green coloured, and starts with massive sandstones that laterally pass to eolianites showing large-scale cross bedding. The last 40 m of the section are characterized by the presence of biotitic air-fall tuffs and reworked pyroclastic deposits, interbedded with tuffaceous, carbonatic mudstones and lutites, sedimented in a lacustrine environment. The deposition of the greenish section finished within the middle Miocene, since a tuff from its upper levels was dated in 12.1 ± 0.7 Ma (K–Ar, Coira et al., in press). This assumption is confirmed through the K–Ar age of 10.3 ± 0.5 Ma of the overlying Orosmayo ignimbrite (Caffe and Coira, 2002). Like the base of the sequence, the younger beds of the Tiomayo Formation show uniform ages across the SJOB, considering that the dates shown above are practically identical to the 12.43 ± 0.08 Ma Ar–Ar age obtained by Ort (1991) from the top of northwesternmost outcrops (Cusi Cusi; Fig. 2A).

Tiomayo Formation beds are subhorizontal, and do not show internal thrusting or compressive faults (Cladouhos et al., 1994), nor even any affection by the largest structure of the region—the San Vicente Thrust—over which the sequence onlaps through 40 km. However, it can commonly be seen tilted by the effects of normal and strike-slip faulting (see Cladouhos et al., 1994; and below).

The Tiomayo Formation does not exhibit continuity north of Panizos, but it would correlate with ∼15 Ma volcanic sequences erupted from Morokho and Bonete volcanoes (Fornari et al., 1993) which crop out farther north, in the South Lipez region.

2.1.2. Casa Colorada volcanic dome complex

The Casa Colorada dacite dome complex is a small extrusive center (∼1.5 km^3) located in the eastern border of SJOB, near Sierra de Rinconada (22°19′S–66°20′W; Fig. 2A). The complex overlies redbeds from the Peña Colorada Formation, as well as the Ordovician basement. Caffe (1996) recognized three successive volcanic events, involving deposition of a tuff ring, collapse of growing lava domes, and effusion of flow-banded dacitic lavas. The 17.3 ± 0.7 Ma K–Ar age of the center (Caffe, 1999), indicates that the main dacite lava dome is somewhat older than the basal units from Tiomayo Formation. This is consistent with its stratigraphic position, since block and ash flow deposits from Casa Colorada underlie an ignimbrite from the Tiomayo Formation reddish section.

2.2. Laguna de Pozuelos basin

The Laguna de Pozuelos basin (Fig. 1) locates in western Cordillera Oriental to the east of the SJOB basin and is separated from the latter by the Sierra de Rinconada range. Its eastern boundary is represented by the Sierra de Escaya, and (to the south) the Sierra de Cochinoca ranges (Fig. 2B). Main outcrops of Cenozoic sedimentary successions include at least four pre-upper Miocene units. The 28–20 Ma Moreta Formation (Coira, 1979; Linares and González, 1990) is a conspicuous, coarse grained intramontane infilling, very similar to those formed contemporaneously in the Bolivian Eastern Cordillera (Kley et al., 1996). The Moreta Formation rocks are followed by the Laguna de Pozuelos volcaniclastic sequence, which comprises alternating pyroclastic and reworked volcanic rocks that crop out in the southwestern border of the Laguna de Pozuelos basin (Fig. 2B). Dated as 18.6 ± 1 Ma (K–Ar, Caffe et al., 2002), it underlies mid-Miocene sediments and tuffs of the Cara Cara strata dated as 14.26 ± 0.19 Ma (Ar–Ar; Cladouhos et al., 1994), therefore correlating with the Tiomayo Formation.

A group of three volcanic dome complexes postdate the latter sequences, and are described in detail as follows.

2.2.1. *Pan de Azúcar (22°36′S; 66°03′W)*

The Pan de Azúcar volcanic dome complex (Fig. 3A) is composed of lava domes, lava flows and a group of pyroclastic units, being erupted from several associated vents in the southern portion of the Laguna de Pozuelos basin (Fig. 2B). The center hosts an important Pb–Zn–Ag(±Sn) ore deposit. Dacitic rocks cover the Ordovician basement, as well as Moreta Formation rocks and Cara Cara strata. Obtained K–Ar ages from Pan de Azúcar rocks (12 ± 2 Ma, 13 ± 1 Ma; Coira, 1979; Linares and González, 1990) allow to situate the complex within the late middle Miocene. Volcanic activity in the region was favoured by NW–SE trending fractures in the Laguna de Pozuelos basin (Coira, 1979; Coira et al., 1996). The evolution of the volcanic center was modelled in three main eruptive stages (Caffe, 2002). First cycle rocks

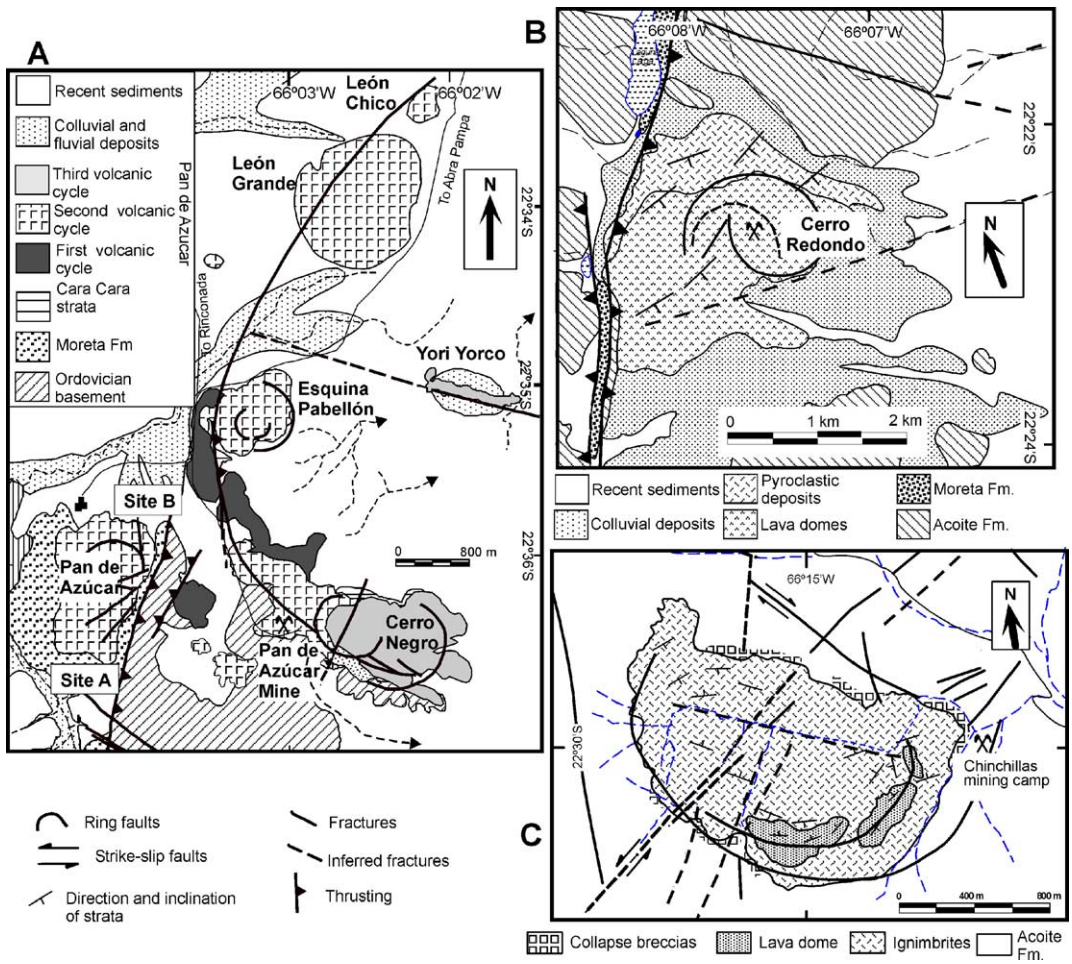

Fig. 3. Volcanic dome complexes in Laguna de Pozuelos basin. (A) Distribution of rocks from different volcanic cycles in Pan de Azúcar. (B) Cerro Redondo eruptive units. (C) Chinchillas volcanic dome complex.

include basal ignimbrites, dacite lavas, hot avalanche and block and ash flow deposits. The second cycle comprises hydromagmatic air-fall tuffs and surge deposits, biotitic dacite lavas and a shallow intrusive body. Most lavas and domes (Pan de Azúcar, Esquina Pabellón, Cerro León Grande and León Chico) erupted during this stage. According to the stratigraphic position, the petrography and the geochemical composition, it is virtually impossible to differentiate more than one magmatic pulse within this group. Nevertheless, using paleomagnetic data at least three distinct pulses can be distinguished (see below). The third volcanic cycle is composed of volcanic breccias, a block and ash flow deposit and dark dacitic lavas, erupted from Cerro Negro and Yori Yorco vents. Besides the stratigraphic situation, the last two units are easily discriminated from previous equivalents by the presence of hornblende as an accesory phase.

2.2.2. Cerro Redondo (22°22′S–66°08′W)

This volcanic dome complex crops out in the eastern border of the Sierra de Rinconada (Fig. 3B), directly overlying the Ordovician basement (Acoite Formation). The only available datation of 12.54 ± 1.1 Ma (apatite fission track) was obtained by Cladouhos et al. (1994). The eruptive history started with the deposition of a thick volcanic breccia—block and ash succession, followed by dacitic lava domes set through a group of nested ring fractures (Caffe, 1999). The main characteristic of this complex is the intense hydrothermal alteration (K–feldspar–sericite–quartz–tourmaline) that affects almost all lavas, reason why we had to discard many of these samples. Instead, block and ash flow deposits show only weak or no alteration, and these were preferentially used in our study. According to Cladouhos et al. (1994), Cerro Redondo rocks show minor deformation in its western boundary, where it is in contact to the San Vicente Thrust (Figs. 2B and 3B), the rest of it remaining rather unaffected.

2.2.3. Chinchillas (22°30′S–66°15′W)

The Chinchillas volcanic dome complex (Fig. 3C) is a small volcanic center located inside the Sierra de Rinconada. The complex has been dated by only a single K–Ar age determination of 13 ± 1 Ma (Linares and González, 1990). The center is set over the Ordovician Acoite Formation, comprising massive low-volume pyroclastic flow deposits, block and ash flow deposits and a dacite lava dome. Like in the Pan de Azúcar case, the eruption of this volcanic structure was related to a NW–SE fracture system.

3. Paleomagnetic sampling

Samples were collected using a portable field drill and oriented using magnetic and solar compasses.

In the San Juan de Oro basin (Fig. 2A) the Tiomayo Formation was sampled in two different localities: Locality A and Locality B (Fig. 2A, Table 1). North of Locality A, in the Casa Colorada volcanic dome complex (Fig. 2A), oriented samples from dacitic lavas were also collected (Table 1).

In the Laguna de Pozuelos basin several dacitic volcanic dome centers, block and ash flow deposits and ignimbrites were paleomagnetically sampled (Figs. 2B and 3, Table 1).

4. Paleomagnetic methods

One to three standard specimens were cut from each sample. Magnetization was measured using a DIGICO spinner magnetometer and a 2G Enterprises cryogenic magnetometer. Detailed alternating field

Table 1
Paleomagnetic sampling

	Number of oriented samples collected	Bedding	
		Strike (°)	Dip (°)
San Juan de Oro basin			
Tiomayo Formation Locality A			
Reddish section	32	60	12
Yellowish section	13	22	5
Greenish section	61	Subhorizontal	
Tiomayo Formation Locality B			
Reddish section	17	0	7
Casa Colorada dacitic dome	9	–	–
Laguna de Pozuelos basin			
Cerro León Chico dacitic dome	9	–	–
Cero León Grande dacitic dome	7	–	–
Cerro Yori Yorco dacitic dome	12	–	–
Cerro Esquina Pabellón dacitic dome	12	–	–
Cerro Negro dacitic dome	7	–	–
Cerro Pan de Azúcar dacitic dome Site A	18	–	–
Cerro Pan de Azúcar dacitic dome Site B	10	–	–
Cerro Pan de Azúcar block and ash flow	11	–	–
Chinchillas ignimbrite 1	7	–	–
Chinchillas ignimbrite 2	5	–	–
Cerro Redondo dacitic dome	6	–	–
Cerro Redondo block and ash flow 1	5	–	–
Cerro Redondo block and ash flow 2	5	–	–

Strike and dip indicate bedding attitude (right-hand rule).

(AF) and thermal demagnetization techniques were applied. With AF up to 18 demagnetization steps were performed, using a 2G600 alternating field demagnetizer up to peak fields of 140 mT. With thermal demagnetization, 18 steps up to temperatures of 700 °C were performed using a Schonstedt TSD-1 furnace. The bulk magnetic susceptibility was measured after each heating step in order to monitor possible magnetic mineral changes. Identification of macroscopic magnetic minerals using polished sections was undertaken. Also, isothermal remanent magnetization (IRM) acquisition, back-field and hysteresis experiments were conducted. For a more conclusive identification of magnetic minerals, bulk magnetic susceptibility (k) versus temperature (T) curves were performed.

Demagnetization results were plotted on vector end point diagrams (Zijderveld, 1967) and equal-angle stereographic projections. The corresponding components of natural remanent magnetization (NRM) were determined using principal components analysis (Kirschvink, 1980; Torsvik, 1992) when linear trends of vector end points were identified. For demagnetization paths trending toward the origin, anchored line fits were applied to isolate characteristic remanent magnetizations (ChRMs). When curved trends of vector end points, or linear trends not going through the origin simultaneously with demagnetization paths on the stereonet were identified, remagnetization circles were obtained. Site-mean directions were determined by combining remagnetization circles and stable end point directions (McFadden and McElhinny, 1988) or applying Fisher's (1953) statistics on end points only. For the calculation of site

Table 2
Paleomagnetic results corresponding to San Juan de Oro basin

Site	Tilt-corrected site-mean directions					Bedding	
	n (n_c)	D (°)	I (°)	α_{95} (°)	κ	Strike (°)	Dip (°)
Reddish section Locality A	7 (32)	6.4	−30.6	9.2	53	60	12
Reddish section Locality B	15 (17)	355.1	−34.4	6.9	34	0	7
Yellowish section	5 (13)	353.1	−34.3	2.2	2611	22	5
Greenish section: BR1	6 (7)	192.3	41.1	20.6	13	Subhorizontal	
Greenish section: BR2	6 (6)	21.8	−36.8	12.6	41	Subhorizontal	
Greenish section: BR3	7 (15)	179.6	33.1	16.1	18	Subhorizontal	
Greenish section: BR4	4 (6)	182.4	29.3	24.9	18	Subhorizontal	
Greenish section: BR5	8 (8)	356.4	−41.6	5.0	124	Subhorizontal	
Greenish section: BR6	5 (9)	169.9	37.1	6.9	263	Subhorizontal	
Casa Colorada dacitic dome	13 (9)	12.6	−30.7	6.2	46	–	–
Mean direction		**3.0**	**−35.3**	**5.6**	**76**		

n (n_c) is number of specimens used in statistic (number of samples collected), D and I are declination and inclination of the mean directions, α_{95} is semiangle of the 95% confidence cone about the mean direction, κ is the precision parameter (Fisher, 1953), strike and dip indicate bedding attitude (right-hand rule).

means only ChRMs with maximum angular deviation <15° were considered. A mean direction was calculated for each basin (San Juan de Oro and Laguna de Pozuelos, Tables 2 and 3) considering site means with $\alpha_{95} < 25°$ and using Fisher's (1953) statistics. The correspondent rotations, inclination flattening and their confidence intervals were calculated in direction space (Demarest, 1983) using as reference the paleopoles determined by Besse and Courtillot (2002).

Table 3
Paleomagnetic results corresponding to Laguna de Pozuelos basin

Site	Location		Site-mean directions				
	Latitude	Longitude	n (n_c)	D (°)	I (°)	α_{95} (°)	κ
Cerro Redondo dacitic dome and two pyroclastic deposits	22°23′S	66°07′W	11 (16)	15.5	−40.7	8.5	30
Chinchillas ignimbrite[a]	22°30′S	66°15′W	5 (5)	183.5	8.4	13.0	46
Cerro León Chico dacitic dome	22°33.5′S	66°01′W	15 (9)	174.6	39.7	4.9	61
Cerro León Grande dacitic dome[a]	22°34′S	66°02.5′W	9 (7)	226.8	46.4	6.6	62
Cerro Yori Yorco dacitic dome	22°35′S	66°01.6′W	12 (12)	7.9	−44.2	2.2	391
Cerro Esquina Pabellón dacitic dome	22°35.2′S	66°03.3′W	12 (12)	18.4	−47.9	4.9	78
Cerro Pan de Azúcar dacitic dome–Site A	22°37′S	66°04.5′W	21 (18)	358.0	−52.7	4.9	44
Cerro Pan de Azúcar dacitic dome–Site B	22°36′S	66°04′W	11 (10)	11.2	−44.1	4.8	92
Cerro Pan de Azúcar pyroclastic deposits	22°37.5′S	66°03.5′W	5 (11)	355.8	−47.0	14.8	33
Mean direction				**5.4**	**−45.9**	**6.0**	**101**

n (n_c) is number of specimens used in statistic (number of samples collected), D and I are declination and inclination of the mean directions, α_{95} is semiangle of the 95% confidence cone about the mean direction, κ is the precision parameter (Fisher, 1953).

[a] Rejected from the mean calculation.

5. Paleomagnetic results

5.1. Tiomayo Formation

5.1.1. Yellowish and greenish sections

Most specimens of the greenish section (45%) and some specimens of the yellowish section (38%) were completely demagnetized after applying temperatures of 400–500 °C or magnetic fields of 40–60 mT. They have demagnetization paths which have both normal and reverse-polarity components (Fig. 4a and b). The normal-polarity magnetizations correspond to an overprint probably due to sample viscosity. Specimens showed either linear nonorigin bound or curved demagnetization paths. It was not possible to isolate individual sample ChRMs and remagnetization circles analysis was used. Some of these specimens underwent a dramatic increase in their bulk magnetic susceptibility (about 150–200%) after heating steps in the range 570–620 °C. The remanent magnetization of a few specimens of the greenish section (20%) showed high unblocking temperatures and high coercivities (Fig. 4c). In most cases a soft component of magnetization was eliminated usually by 10–15 mT or 250–300 °C. Above these demagnetization levels, specimens showed linear demagnetization paths trending toward the origin from which normal or reverse characteristic components were isolated. The bulk magnetic susceptibility of these specimens remained almost constant during successive thermal demagnetization steps. Most specimens of the yellowish section (62%) and some specimens of the greenish section (35%) showed random behavior upon thermal and/or AF demagnetization and were rejected.

5.1.2. Reddish section

Specimens could not be demagnetized by AF; thermal demagnetization was applied. Some of them (36%) were completely demagnetized after applying temperatures of 600–660 °C. They have demagnetization paths which have both normal and reverse-polarity components (Fig. 4d and e). The normal-polarity magnetizations correspond to an overprint probably due to sample viscosity. Specimens showed either linear nonorigin bound or curved demagnetization paths. It was not possible to isolate individual sample ChRMs and remagnetization circles analysis was used. Some of these specimens underwent a dramatic increase in their bulk magnetic susceptibility (about 150–200%) after heating steps in the range 620–640 °C. The remanent magnetizations of a few specimens (8%) are single component (Fig. 4f). Such specimens showed linear demagnetization paths trending toward the origin from which normal characteristic components were isolated. Their bulk magnetic susceptibility remained almost constant during successive thermal demagnetization steps. Most specimens of this section (56%) showed random behavior upon thermal demagnetization and were rejected.

5.2. Volcanic dome complexes

The remanent magnetizations of some specimens (32%) are single component and show high unblocking temperatures and high coercivities (Fig. 5a). Such specimens showed linear demagnetization paths trending toward the origin from which normal and reverse characteristic components were isolated.

Most of the specimens (43%) showed a soft component of magnetization that was eliminated usually by 10–30 mT or 300–600 °C (Fig. 5b). Above these demagnetization levels, specimens showed linear demagnetization paths trending toward the origin from which normal or reverse characteristic components were isolated.

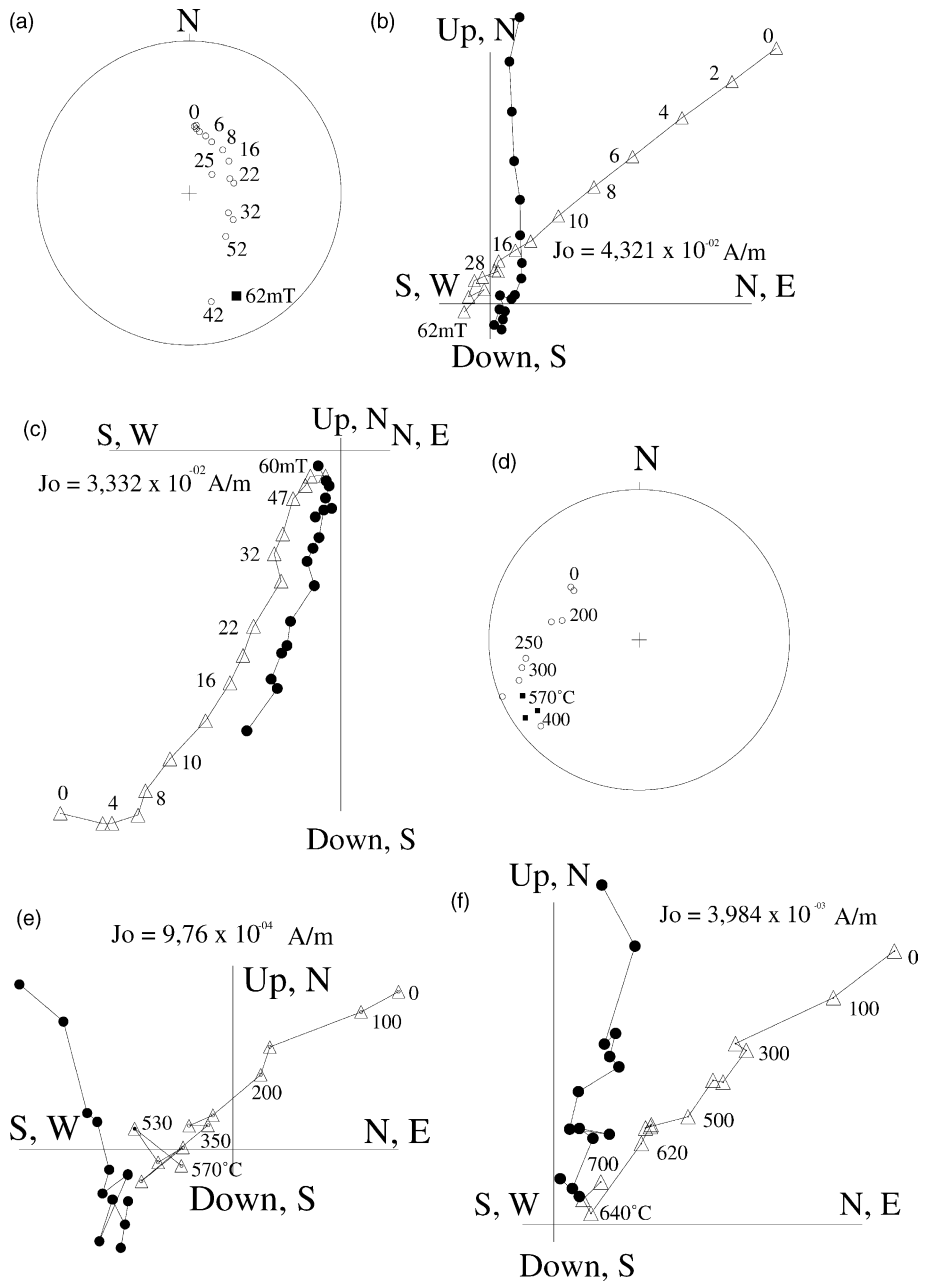

Fig. 4. Examples of typical demagnetization behavior of rocks from the Tiomayo Formation. Specimens of the greenish section: (a) and (b) BR7-2, (c) BR13-2. Specimens of the reddish section: (d) and (e) SA3-1, (f) SA8-1. In the orthogonal plots, solid circles (open triangles) indicate horizontal (vertical) projection. In the stereoplot, open symbols (solid) indicate negative (positive) inclination.

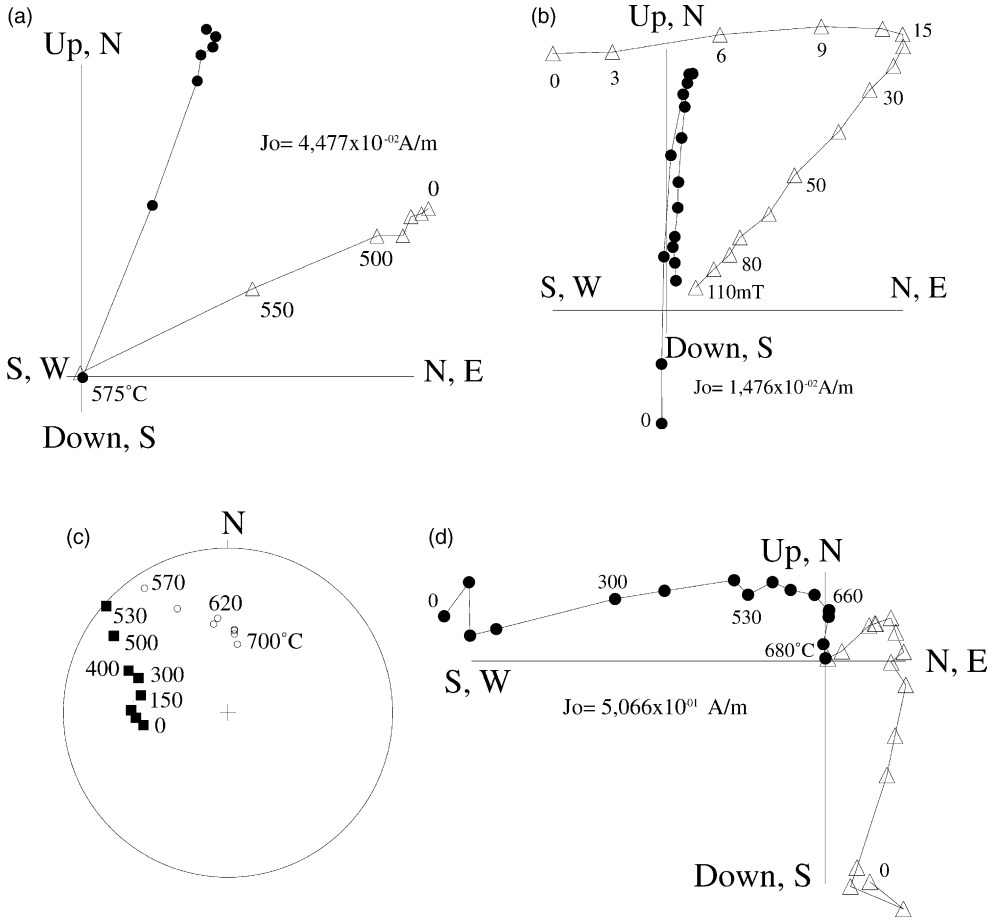

Fig. 5. Examples of typical demagnetization behavior of rocks from dacitic volcanic dome complexes. Specimen of Casa Colorada dacitic dome: (a) CC4-1. Specimen of Cerro Pan de Azúcar dacitic dome (Site B): (b) PA27-1. Specimen of Cerro Pan de Azúcar dacitic dome (Site B): (c) and (d) CL18-1. Convention in orthogonal plots and stereonet as in Fig. 4.

Few specimens (7%) have demagnetization paths which have both normal and reverse-polarity components (Fig. 5c and d). They showed curved demagnetization paths. It was not possible to isolate individual specimen ChRMs and remagnetization circles analysis was used.

Some specimens (18%) were rejected because of either random behavior upon demagnetization or dramatic bulk magnetic susceptibility increases during thermal demagnetization.

6. Magnetic mineralogy

6.1. Tiomayo Formation

The experiments of IRM acquisition and back-field showed that the main carrier of the remanence in the reddish section's specimens is hematite (Fig. 6). The steep slope of the curve in the first steps suggests

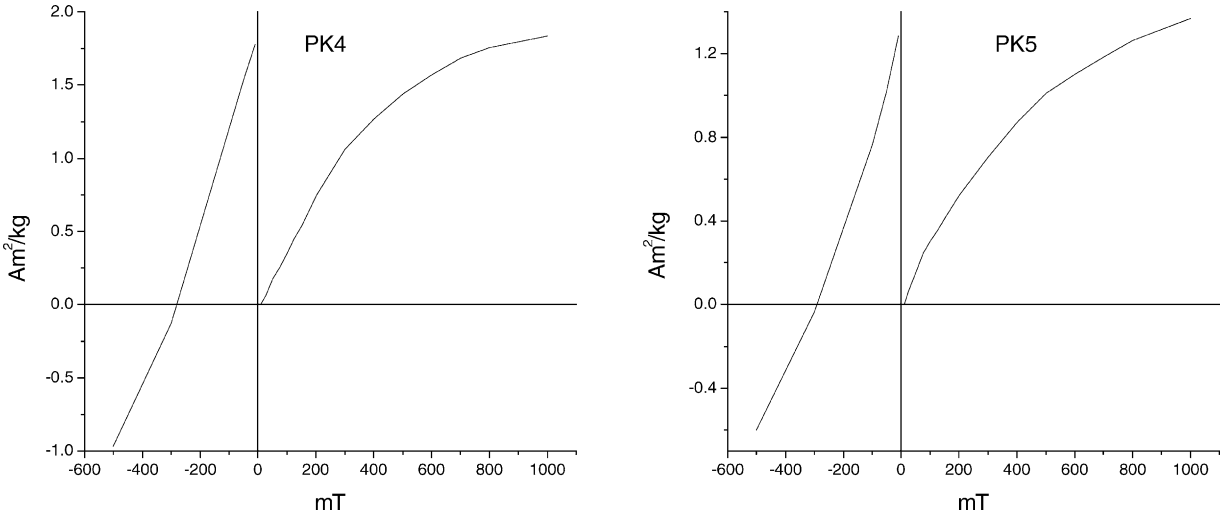

Fig. 6. Experiments of IRM acquisition and back-field corresponding to specimens of the reddish section of the Tiomayo Formation, sampled in Locality B.

the additional presence of some (titano)magnetite. Hysteresis cycles and bulk magnetic susceptibility (k) versus temperature (T) curves were very poorly defined due to the low values of susceptibility and the low content of (titano)magnetite. For the greenish section's samples, experiments of IRM acquisition and back-field and hysteresis cycles (Fig. 7) indicated that the main carrier of the isolated magnetization is (titano)magnetite. Bulk magnetic susceptibility (k) versus temperature (T) curves (Fig. 8) showed that the Curie temperature ranges between 400 and 550 °C, suggesting that such (titano)magnetites would have high content of Ti or large grain size.

In some specimens belonging to the reddish section scarce moderately rounded to rounded (titano) magnetite grains of nearly 50–70 μm in diameter together with abundant hematitic pigment were observed in polished sections. In some specimens corresponding to the greenish section, the presence of moderately rounded to rounded grains of titanomagnetites with high Ti content was determined in polished sections. Such grains have diameters ranging between 30 and 150 μm and show high-temperature oxidation (Haggerty, 1991). Ilmeno-hematite trellis lamellae intergrowths along the {1 1 1} planes were observed in most titanomagnetite grains. Stages of oxidation range from C1 to C7 (Haggerty, 1991). Sandwich and composite oxidation textures were also found. No evidence of low-temperature oxidation (limonitization, maghemitization) was detected. The titanomagnetites observed would correspond to multidomain grain size, but the trellis lamellae divide the grains into isolated smaller magnetic sectors of titanomagnetite poorer in Ti (the Ti being concentrated in the illmenite lamellae). Therefore, the stability of the magnetization could be increased, and some grains could show pseudo-single domain characteristics. Through the observation of thin sections, it was determined that the specimens of the reddish section have hematite as cement, while the specimens of the greenish section have chlorite as cement. These observations coincide with the behaviour shown by the specimens upon thermal and AF demagnetization and with the results obtained from bulk magnetic susceptibility (k) versus temperature (T) curves, IRM acquisition, back-field and hysteresis experiments.

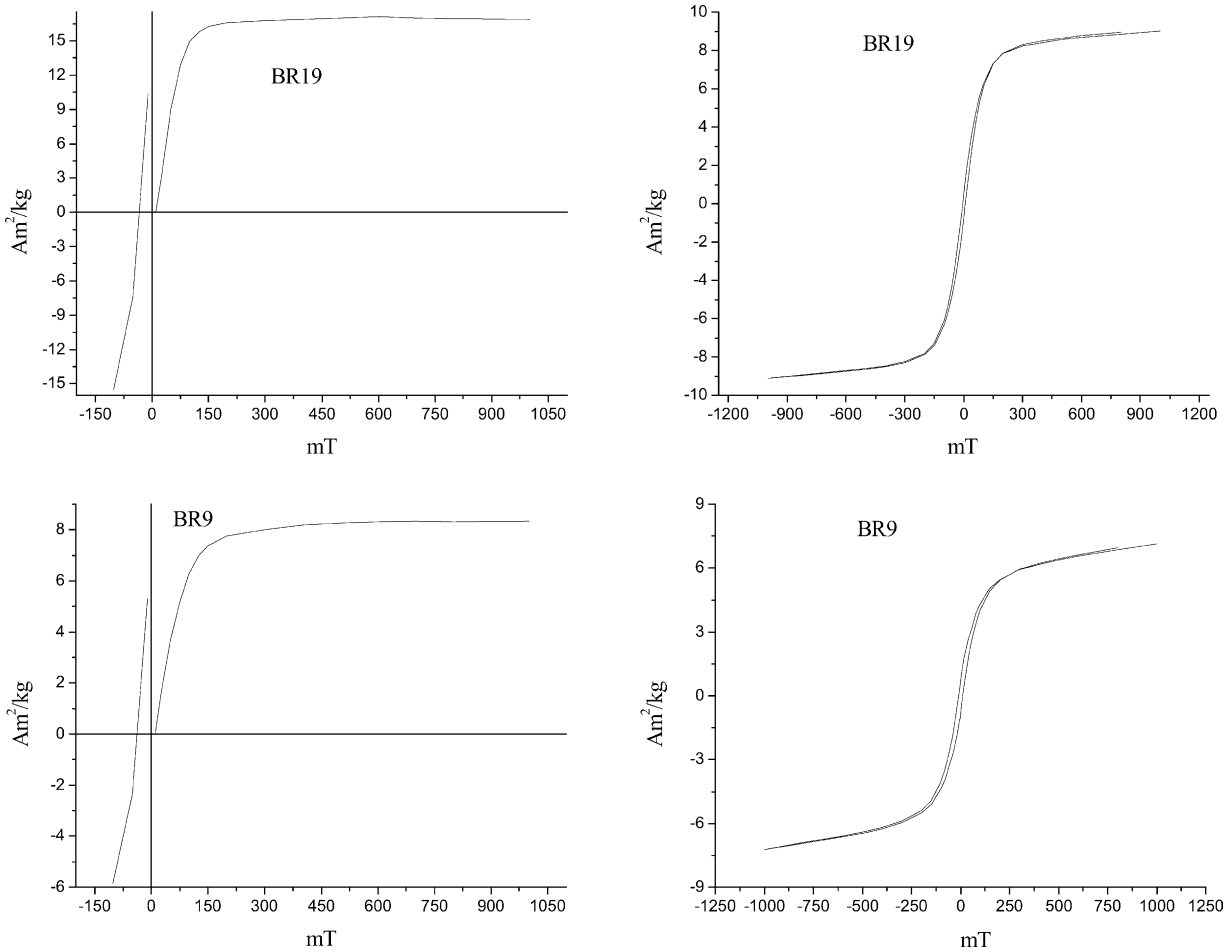

Fig. 7. Experiments of IRM acquisition and back-field (left column) and hysteresis curves (right column) corresponding to specimens of the greenish section of the Tiomayo Formation.

6.2. Volcanic dome complexes

Experiments of IRM acquisition and back-field and hysteresis cycles (Fig. 9) indicated that the main carrier of the isolated magnetizations is (titano)magnetite, hematite being not detected. Bulk magnetic susceptibility (k) versus temperature (T) curves (Fig. 10) showed that the Curie temperature ranges between 500 and 570 °C, suggesting that such (titano)magnetites would have low content of Ti.

The Casa Colorada lavas have abundant oxide minerals, either as inclusions in all major phases (feldspars, quartz, biotite or hornblende) or as microlites in matrix glasses. Rather large cubic crystals of titanomagnetite (50–300 μm) show uniform aspects (C1 stage), without any sign of oxidation-exsolution, averaging compositions (Caffe et al., 2002) between 18 and 21 mol% of the ülvospinel component (Fe_2TiO_4). Subordinate ilmenite could be found only as small stretched inclusions in plagioclase borders and quartz. Ilmenite exhibits up to 7–18 mol% of the hematite component, and only 1 mol% of

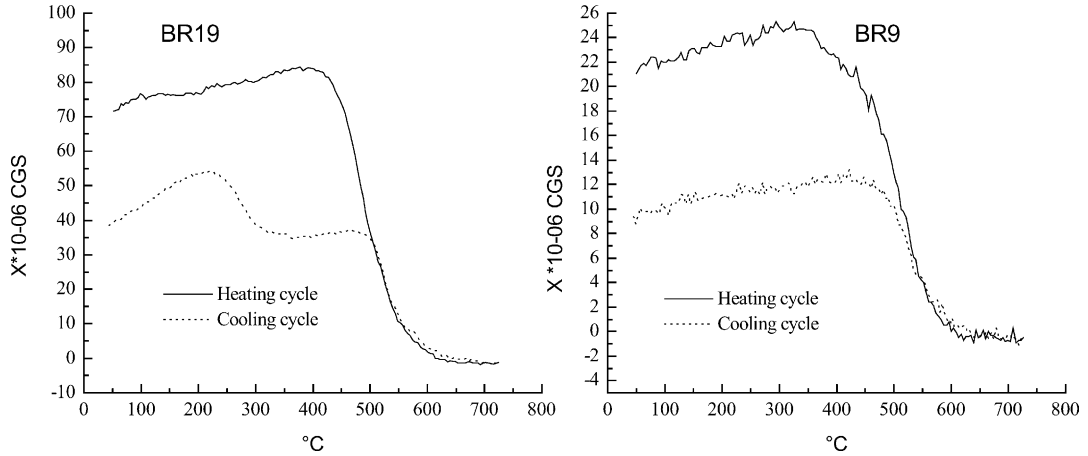

Fig. 8. Bulk magnetic susceptibility (k) vs. temperature (T) curves corresponding to specimens of the greenish section of the Tiomayo Formation.

the geikielite ($MgTiO_3$) and pyrophanite ($MnTiO_3$) end-members; oxidation was weak since rutile and titanohematite are always absent (R1 stage of Haggerty, 1991).

Lavas from different cycles in Pan de Azúcar can be distinguished using the oxide mineralogy: second cycle rocks show scarce and small (5–20 μm) oxide crystals, ilmenite being much more abundant than titanomagnetite; instead, third cycle lavas have oxides with a larger grain size (35–500 μm), and show predominating titanomagnetite. Nevertheless, in both cases the petrographic characteristics are very similar. Single ilmenite crystals are restricted to inclusions in feldspar cores, meanwhile cubic shaped titanomagnetite can be included in plagioclase, biotite, hornblende or as microlites or microphenocrysts in matrix glasses. Almost all Pan de Azúcar titanomagnetite is affected by oxidation at high-temperature, and only a few crystals coming from Cerro Negro and Yori Yorco domes have rather homogeneous aspects (C1–C2 stages), which translate into ülvospinel contents of around 23–29 mol% (Caffe et al., 2002). However, most crystals show trellis textures, compatible with C2–C3 stages of Haggerty (1991) classification. Trellis textured titanomagnetite involves a complex intergrowth of pure ilmenite and Ti-poor (<2 mol% ülvospinel) magnetite lamellae. Primary ilmenite often has rather low hematite contents (2–14 mol%), but in some lava flows from the third cycle it shows intense oxidation textures, and transformation to a rutile–titanohematite intergrowth.

In polished samples from Cerro Redondo lavas, Brito and Sureda (1992) found homogeneous (titano)magnetite, but it remains unclear if it is primary or related to the mineralization event.

7. Analysis of the obtained results

7.1. San Juan de Oro basin

Unit-weighted specimens were used in calculating site means. Such site means were obtained applying Fisher's (1953) statistics or the methods of Halls (1976) and/or of McFadden and McElhinny (1988). When the last two methods were combined, the first one was used to estimate the most probable site-mean

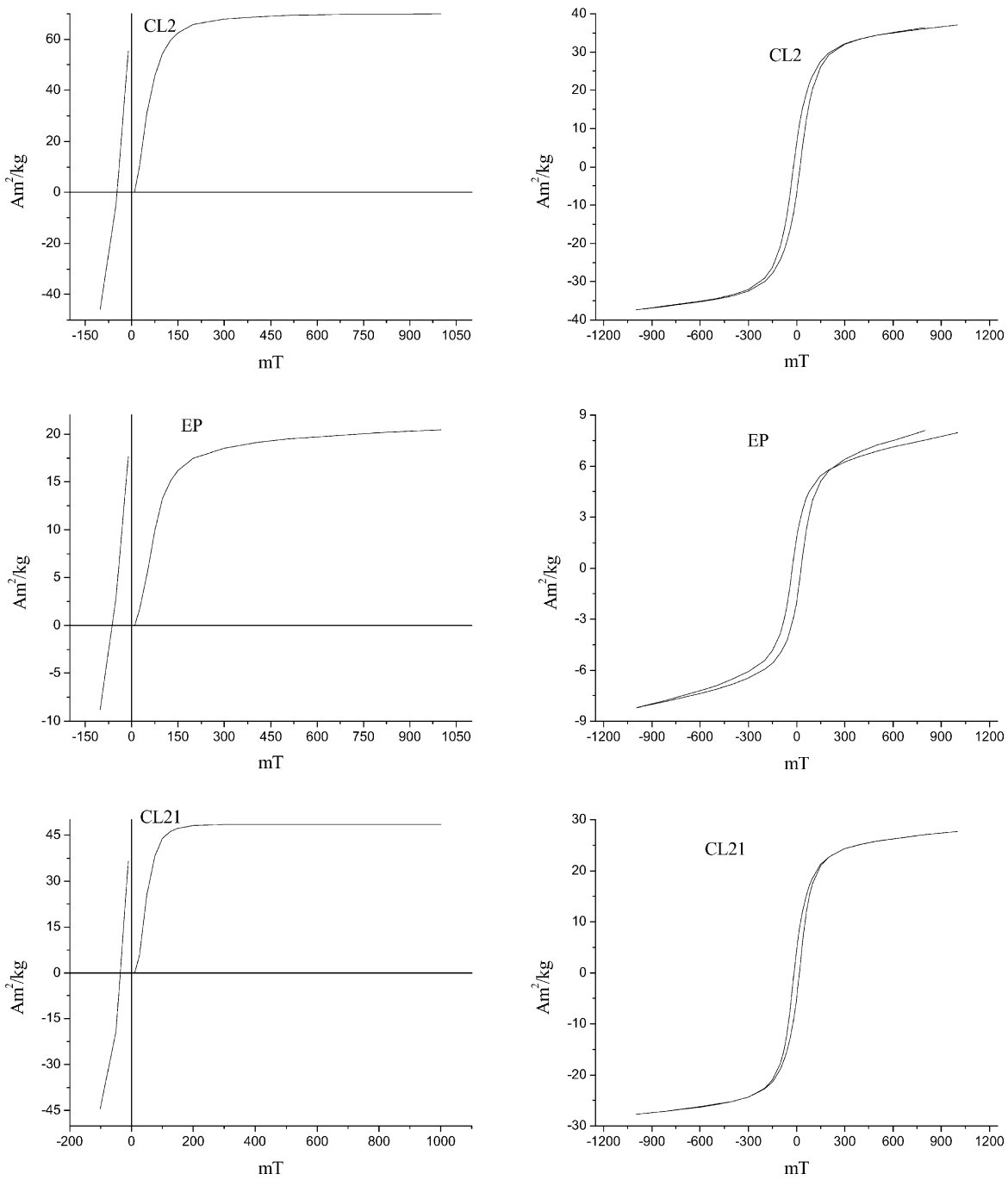

Fig. 9. Experiments of IRM acquisition and back-field (left column) and hysteresis curves (right column) corresponding to specimens of different volcanic complexes. CL2: Cerro León Grande dacitic dome. EP: Cerro Esquina Pabellón dacitic dome. CL21: Cerro Pan de Azúcar dacitic dome (Site B).

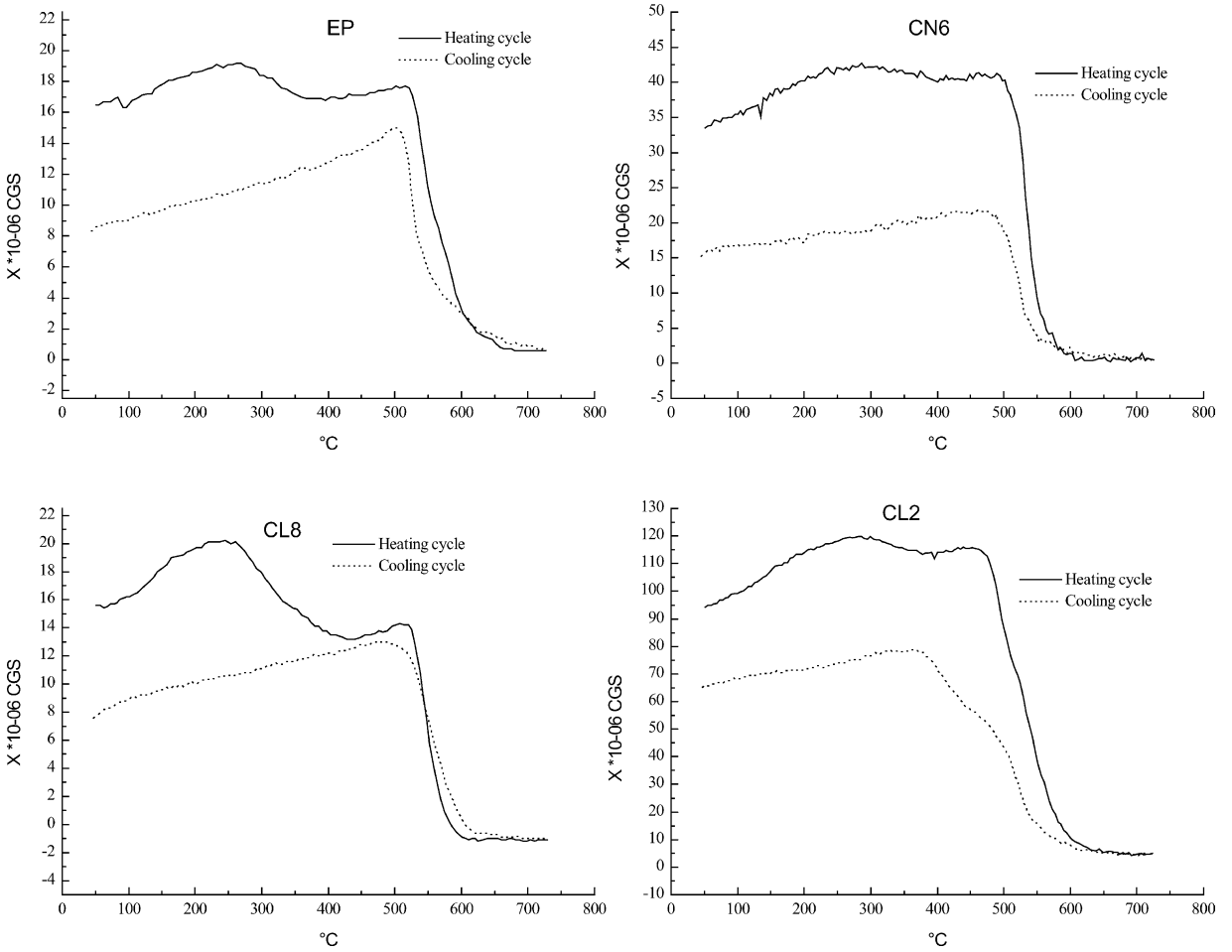

Fig. 10. Bulk magnetic susceptibility (k) vs. temperature (T) curves corresponding to specimens of different volcanic complexes. CN6: Cerro Negro dacitic dome. EP: Cerro Esquina Pabellón dacitic dome. CL8: Cerro León Chico dacitic dome. CL2: Cerro León Grande dacitic dome.

directions. Afterwards, such estimated directions and the remagnetization circles were used with the second method to obtain the true site-mean directions (the estimated directions were subtracted from the directions calculated after the first loop of the iteration).

Tiomayo Formation: considering the high number of specimens rejected due to random behavior, a single site-mean direction was calculated for the yellowish section and two site means were obtained for the reddish section, one for each sampled locality (Table 2). For the greenish section, six site means were determined (Table 2). The site-mean directions have positive and negative inclinations (Table 2), so the reversal test (McFadden and McElhinny, 1990) was performed using simulation. With the tilt-corrected site-mean directions the angle between the mean of the normal-polarity set and the mean of the reverse-polarity set was 1.4° and the critical angle was 12.4° ($N = 9$). The test was successful with classification C. This positive reversal test supports the idea that there is no bias due to inappropiate analysis or deficient

demagnetization and that overall site-mean directions fully average secular variations and reflect an axial dipole field. The fold test (McFadden, 1990) was also performed, but it was statistically indetermined, probably due to the low dip of the sampled beds.

Casa Colorada volcanic complex: considering that the Casa Colorada volcanic dome center is located in the San Juan de Oro basin and that it is broadly similar in age to the lower member of the Tiomayo Formation, the site-mean direction corresponding to Casa Colorada dacitic dome (Table 2) was combined with the site-mean directions calculated for the Tiomayo Formation.

Therefore a single mean direction was calculated (Table 2). The correspondent rotation and inclination flattening are:

$$R \pm \Delta R = 5.2 \pm 6.5^{\circ}$$

$$F \pm \Delta F = -9.8 \pm 6.4^{\circ}$$

This mean direction shows statistically significant inclination flattening, suggesting that perhaps Tiomayo Formation sedimentary rocks underwent post-depositional compaction or other depositional processes (e.g. gravitational forces acting during deposition).

7.2. Laguna de Pozuelos basin

Unit-weighted specimens were used in calculating site means. Such site means were obtained applying the method of McFadden and McElhinny (1988) or Fisher's (1953) statistics (Table 3).

For Cerro Redondo a single site-mean direction was calculated combining the ChRMs determined from the block and ash flow deposit and the dacitic lava samples, considering that they showed very similar declination and inclination values. In the case of the volcanic dome center cropping out in Chinchillas, a site mean was obtained for one of the two ignimbrites sampled. Most of the specimens from the other ignimbrite were rejected because of dramatic bulk magnetic susceptibility increases during heating or random behavior. The specimens collected from Cerro Negro (part of the Pan de Azúcar dome complex) were also rejected because the directions of the remagnetization circles and the ChRMs isolated were discordant amongst themselves, so it was not possible to calculate a reliable site-mean direction. In addition, the site-mean directions corresponding to the Cerro León Grande dacitic dome and to the Chinchillas ignimbrite were not considered in the following analysis because they are markedly removed from the remaining site means. It was determined through the application of a statistical test (Fisher et al., 1981) that such site-mean directions do not belong to the population of site-mean directions obtained for the Laguna de Pozuelos basin (Table 3).

The site-mean directions have positive and negative inclinations (Table 3), so the reversal test (McFadden and McElhinny, 1990) was performed as an isolated observation test. The angle between the mean of the normal-polarity set and the reverse-polarity direction was 11.7° and the critical angle was 16.2° ($N = 7$). The test was successful with classification CI. This positive reversal test supports the idea that there is no bias due to inappropiate analysis or deficient demagnetization and that overall site-mean directions fully average secular variations and reflect an axial dipole field. Furthermore, the fact that the site means obtained for the different volcanic dome centers show different polarities and directions, suggests that such volcanic centers are not coeval and do not belong to a single magmatic event. Particularly, it could be determined that the dacitic volcanic dome centers of Cerro León Chico, Cerro León Grande and Cerro Pan de Azúcar – Esquina Pabellón were not emplaced simultaneously and do not correspond to the same vol-

canic episode. According to the stratigraphic position, the petrography and the geochemical composition, it is virtually impossible to differentiate more than one magmatic pulse within this group. Nevertheless, using paleomagnetic data at least three distinct pulses can be distinguished. While site means with negative inclination have been calculated for Cerro Pan de Azúcar and Esquina Pabellón domes and pyroclastic deposits (Table 3), site means with positive inclination and statistically distinct declination correspond to Cerro León Grande and Cerro León Chico volcanic complexes (Table 3), suggesting the existence of at least three different magmatic episodes.

A single mean direction was calculated (Table 3). The correspondent rotation and inclination flattening are:

$$R \pm \Delta R = 7.6 \pm 7.8^{\circ}$$

$$F \pm \Delta F = 0.8 \pm 6.8^{\circ}$$

This mean direction shows statistically insignificant inclination flattening. Considering that only volcanic rocks were sampled in Laguna de Pozuelos basin, this fact would support the above proposed hypothesis to explain the inclination shallowing showed by San Juan de Oro basin mean direction.

8. Discussion and conclusions

Our results show very low, statistically insignificant rotation in middle Miocene rocks from the northern Puna and western Cordillera Oriental in northwestern Argentina. Upper Miocene (10 Ma and younger) ignimbrites, which overlie these middle Miocene rocks, are unrotated (Table 4, see also Somoza et al., 1996). Then, integrated paleomagnetic data from Neogene rocks in the studied area, suggest the possibility of the existence of very low rotation during middle Miocene, since results from the overlying ignimbrites indicate that rotational deformation shut down by the late Miocene.

The observations may be extended in space when available paleomagnetic data from coeval rocks in neighbouring areas of the Altiplano-Puna and western Cordillera Oriental are considered (Table 4). About

Table 4
Paleomagnetic data considered in Section 8

	Age (Ma)	Location		$R \pm \Delta R$ (°)	Reference
		Latitude (°S)	Longitud (°W)		
Upper Miocene ignimbrites	10	22.5	66.7	−0.3 ± 9.5 (1)	Somoza et al. (1996)
Morro Blanco	10	23	66.5	−0.9 ± 4.8 (1)	Prezzi and Alonso (2002)
Laguna de Pozuelos basin	12	22.4	66	7.6 ± 7.8 (1)	This study
San Juan de Oro basin	13	22.5	66.5	5.2 ± 6.5 (1)	This study
Quebrada Honda	13	22	65.5	19.9 ± 5.6 (1)	MacFadden et al. (1990)
Cerdas	16	21.8	66.3	12.4 ± 8.1 (2)	MacFadden et al. (1995)
Lipez Sediments	20	21.8	66.5	10.8 ± 17.7 (3)	Roperch et al. (2000)
Lipez Rondal volcanics	20	21.8	66.5	40.3 ± 12.2 (3)	Roperch et al. (2000)

Age indicates the approximate age of the magnetization. Location indicates the geographic coordinates of the respective sampling area. $R \pm \Delta R$ are rotation (clockwise positive) and confidence interval in direction space (Demarest, 1983) using as reference the paleopoles determined by Besse and Courtillot (2002): (1): 10 Ma paleopole, (2): 15 Ma paleopole, (3): 20 Ma paleopole.

60 km southeast of the study area, unrotated 10 Ma rocks at Morro Blanco (Prezzi and Alonso, 2002) have a tectonic significance similar to that of the unrotated upper Miocene ignimbrites above mentioned (Table 4). On the other hand, about 60–100 km north, probable lower Miocene sedimentary rocks at Lipez show low, statistically insignificant rotation (Roperch et al., 2000) (Table 4), a result compatible with those from the Laguna Pozuelos and San Juan de Oro basins reported here. Similarly, low magnitude rotation was reported for the 16–15 Ma Cerdas section (MacFadden et al., 1995) (Table 4) which is located in the eastern border of the Bolivian Altiplano, close to the international boundary. Despite their low values, all of the declination anomalies found from rocks older than 10 Ma in Table 4 are positive. This is true even when comparing the data to Neogene reference poles others than the used in Table 4. Although we cannot rule out the possibility that uncompleted sampling of the paleofield could affect some of these results, such a deficiency in the data would more likely produce a random between-locality dispersion of the mean directions, rather than the systematic clockwise biasing observed. Thus, paleomagnetic results from rocks older than 10 Ma distributed along a ca. 100 km stripe in the western border of the Altiplano-Puna, suggest the occurrence of a pre-late Miocene clockwise rotation of low magnitude.

Contrasting with these results, Roperch et al. (2000) showed that the lower Miocene Rondal volcanics at Lipez underwent about 40° clockwise rotation (Table 4). These authors proposed that this large rotation is of local origin, related to tectonic activity in both the San Vicente Thrust and the Pululus fault zone, two tectonic features surrounding the Rondal locality. Our results further support the interpretation that the large rotation in the Rondal lavas reflects just local tectonic conditions.

The paleomagnetic data from this latitudinal stripe of the southern Central Andes may be analyzed in the context of thrust deformation. The main fault in the study area, the west vergent San Vicente Thrust, was active during late Oligocene–early Miocene times (Müller et al., 2002). Undeformed, ca. 17 Ma ignimbrites that cover this thrust and associated sedimentary deposits in the Bolivian sector indicate end of fault motion by the late early Miocene (Müller et al., 2002). Likewise, on the basis of a local unconformity observed in the northern Puna, Caffe and Coira (2002) suggested that the motion of this fault stopped between 18 and 15 Ma. Then, major activity in the San Vicente Thrust pre-dates many of the paleomagnetically studied units in this region. In the preceding paragraph we showed that paleomagnetic results in the region point out to the possibility that a low magnitude, clockwise rotation could have affected rocks older than 10 Ma listed in Table 4. If so, cross relations suggest that the low magnitude rotation occurred after the motion in the San Vicente Thrust largely ceased, arguing against a direct link between local fault activity and rotation. To the east of the study area, however, faulting in most of the Cordillera Oriental at these latitudes continued during the middle Miocene. The results of this crossing between paleomagnetic and structural data agree with the model of Müller et al. (2002), who envisaged that active middle Miocene thrusting in the Cordillera Oriental east of the analyzed region accommodated passive rotations in the mostly tectonically inactive internal areas (see Fig. 17c in Müller et al., 2002). However, this kind of models also requires passive rotation of the forearc at these latitudes (e.g. Isacks, 1988; Kley, 1999) in contrast with paleomagnetic results from lower Miocene rocks in the forearc, which indicate negligible Neogene rotation (Roperch et al., 2000; Somoza and Tomlinson, 2002). These apparently conflictive observations remark the still scarce paleomagnetic and structural information to model the Neogene evolution of the Central Andes.

The unrotated upper Miocene (10 Ma and younger) ignimbrites represent the end of rotational deformation in the study area. These ignimbrites constitute a physical expression of the San Juan del Oro Surface (SJOS, see Gubbels et al., 1993), an undeformed unconformity/erosional surface which cuts across regional Eocene to middle Miocene shortening structures over much of the Cordillera Oriental/Altiplano-

Puna. The SJOS does not extend farther east than the eastern part of the Cordillera Oriental (Gubbels et al., 1993). Eastward of the Cordillera Oriental, shortening in the external part of the orogen (Subandean belt) largely started at times of SJOS formation and is still going on. Relevant paleomagnetic data from the 13–12 Ma Quebrada Honda section (MacFadden et al., 1990), located in the easternmost border of the Cordillera Oriental, indicate clockwise rotation of about 20° (Table 4) associated with a transfer zone in the Subandean belt (Somoza et al., 1999). The development of this transfer zone, and by inference, of the associated rotation in the Quebrada Honda section, is likely younger than the development of the SJOS (Kley, 1996). This suggests that, close to the time when rotational deformation ceased in the Altiplano-Puna, the external part of the orogen started to rotate. This is in agreement with paleomagnetic observations from the forearc, which suggest that significant tectonic rotations roughly encompass the variable timing of local contractional deformation in the southern Central Andes (Roperch et al., 2000; Somoza and Tomlinson, 2002).

Acknowledgements

C. Prezzi gratefully acknowledges the support of an Alexander von Humboldt Research Fellowship from the Alexander von Humboldt Foundation, during which this paper was finished. Many of the magnetic mineralogy measurements and experiments were performed in the Instituto Astronomico e Geofisico, Universidade de Sao Paulo, Brazil. We thank Andrés Tassara for helpful discussion.

References

Beck, M., 1998. On the mechanism of crustal block rotations in the central Andes. Tectonophysics 299, 75–92.

Bellman, R.N., Chomnales, R., 1960. Estudio hidrogeológico del Valle de Puesto Grande y sus posibilidades económicas. Acta Geológica Lilloana 3, 191–226. Tucumán.

Besse, J., Courtillot, V., 2002. Apparent and true polar wander and the geometry of the geomagnetic field over the last 200 Myr. J. Geophys. Res. 107 (B11), 2300, doi: 10.1029/2000JB000050.

Brito, J., Sureda, R., 1992. Exploración del Prospecto Polimetálico Cerro Redondo, Rinconada, Jujuy, Argentina. Actas IV Congreso Nacional de Geología Económica, pp. 183–194, Córdoba.

Caffe, P.J., 1996. La dacita de Casa Colorada. Complejo volcánico dómico del Terciario superior en Puna Norte, Argentina. Memorias del XII Congreso Geológico de Bolivia Tomo III, pp. 1019–1030, Tarija, Bolivia.

Caffe, P.J., 1999. Complejos volcánicos dómicos del Terciario superior de Puna Norte: sus implicancias magmatotectónicas y metalogenéticas. Ph.D. Thesis. Facultad de Ciencias Exactas, Físicas y Naturales, Universidad Nacional de Córdoba, Argentina, 421 pp.

Caffe, P.J., 2002. Estilos eruptivos del complejo volcánico dómico Pan de Azúcar – Puna Norte. Revista de la Asociación Geológica Argentina 57 (3), 232–250.

Caffe, P.J., Coira, B.L., 2002. Chronostratigraphy of the San Juan de Oro basin and its tectonic implications for the northern Puna during the Miocene. 5th International Symposium on Andean Geodynamics Abstract volume Congress, pp. 109–112. Toulouse, France.

Caffe, P.J., Trumbull, R.B., Coira, B.L., Romer, R.L., 2002. Petrogenesis of Early Neogene magmatism in the Northern Puna; implications for magma genesis and crustal processes in the Central Andean Plateau. J. Petrol. 43, 907–942.

Carey, S., 1958. The tectonic approach to continental drift. In: Carey, S. (Ed.) Continental Drift—A Symposium. University of Tasmania Press, Hobart, Tasmania, pp. 178–355.

Cladouhos, T.T., Allmendinger, R.W., Coira, B., Farrar, E., 1994. Late Cenozoic deformation in the Central Andes: fault kinematics from the northern Puna, northwestern Argentina and southwestern Bolivia. J. South Am. Earth Sci. 7 (2), 209–228.

Coira, B., 1979. Descripción Geológica de la Hoja 3c, Abra Pampa, Pcia. de Jujuy. Boletín del Servicio Geológico Argentino 170, 1–90.

Coira, B., Kay, S., Viramonte, J., 1993. Upper Cenozoic magmatic evolution of the Argentine Puna—a model for changing subduction geometry. Int. Geol. Rev. 35, 677–720.

Coira, B., Caffe, P., Soler, M., 1996. Interpretación geológica del relevamiento aeromagnético de la Puna Septentrional, Jujuy y Salta. II. Area Depresión de Pozuelos. II.1-Geología y minería. Dirección Nacional del Servicio Geológico Serie Contribuciones técnicas (1). Geofísica, pp. 11–13. Buenos Aires.

Coira, B., Caffe, P.J., Ramírez, A., Chayle, W., Díaz, A., Rosas, S.A., Pérez, A., Pérez, E.M.B., Orosco, O., Martínez, M., Hoja Geológica 2366-I Mina Pirquitas (1:250.000). SEGEMAR, Secretaría de Minería de la Nación, Argentina, in press.

Demarest, H., 1983. Error analysis for the determination of tectonic rotation from paleomagnetic data. J. Geophys. Res. 88, 4321–4328.

de Silva, S.L., 1989. The Altiplano-Puna volcanic complex of the central Andes. Geology 17, 1102–1106.

Fisher, R., 1953. Dispersion on a Sphere. Proc. R. Soc. London, Ser. A 217, 295–305.

Fisher, N.I., Lewis, T., Willcox, M.E., 1981. Tests of discordancy for samples from Fisher's distribution on the sphere. Appl. Stat. 30, 230–237.

Fornari, M., Pozzo, L., Soler, P., Bailly, L., Leroy, J., Bonhomme, M.G., 1993. Miocene volcanic centers in the southern Altiplano of Bolivia, The Cerro Morokho & Cerro Bonete area (Sur lípez). Second International Symposium on Andean Geodynamics, Oxford (UK), Abstract Volume. ORSTOM, pp. 363–366.

Gubbels, T., Isacks, B., Farrar, E., 1993. High-level surfaces, plateau uplift, and foreland development, Bolivian Central Andes. Geology 21, 695–698.

Haggerty, S., 1991. Oxide textures—a Mini Atlas. In: Lindsley, D.H. (Ed.), Oxide Minerals: Petrologic and Magnetic Significance; Rev. in Miner. 25, 129–219.

Halls, H.C., 1976. A least squares method to find a remanence direction from converging remagnetization circles in paleomagnetism. Phys. Earth Planet. Interiors 16, 1–11.

Isacks, B.L., 1988. Uplift of the Central Andean Plateau and bending of the Bolivian Orocline. J. Geophys. Res. 93, 3211–3231.

Kirschvink, J.L., 1980. The least-squares line and plane and the analysis of palaeomagnetic data. Geophys. J. R. Astron. Soc. 62, 699–718.

Kley, J., 1996. Transition from basement-involved to thin-skinned thrusting in the Cordillera Oriental of southern Bolivia. Tectonics 15 (4), 763–775.

Kley, J., 1999. Geologic and geometric constraints on a kinematic model of the Bolivian orocline. J. South Am. Earth Sci. 12, 221–235.

Kley, J., Muller, J., Tawackoli, S., Jacobshagen, V., Manutsoglu, E., 1996. Pre-Andean and Andean-age deformation in the Eastern Cordillera of Southern Bolivia. J. South Am. Earth Sci. 10, 1–19.

Linares, E., González, R.R., 1990. Catálogo de edades radiométricas de la República Argentina 1957–1987. Asociación Geológica Argentina, Publicaciones Especiales 19, 628 pp.

MacFadden, B., Anaya, F., Swisher Jr., C., 1995. Neogene paleomagnetism and oroclinal bending of the central Andes of Bolivia. J. Geophys. Res. 100 (B5), 8153–8167.

MacFadden, B., Anaya, F., Perez, H., Naeser, C., Zeitler, P., Campbell, K., 1990. Late Cenozoic paleomagnetism and chronology of Andean basins of Bolivia: evidence for possible oroclinal bending. J. Geol. 98, 541–555.

McFadden, P.L., 1990. A new fold test for paleomagnetic studies. Geophys. J. Int. 103, 163–169.

McFadden, P.L., McElhinny, M.W., 1988. The combined analysis of remagnetization circles and direct observations in palaeomagnetism. Earth Planet. Sci. Lett. 87, 161–172.

McFadden, P.L., McElhinny, M.W., 1990. Classification of the reversal test in palaeomagnetism. Geophys. J. Int. 103, 725–729.

Müller, J., Kley, J., Jacobshagen, V., 2002. Structure and Cenozoic kinematics of the Eastern Cordillera, southern Bolivia (21°S). Tectonics 21(5), doi: 10.1029/2001TC001340.

Ort, M.H., 1991. Eruptive dynamics and magmatic processes of Cerro Panizos, Andes. Ph.D. thesis, University of California, Sta. Barbara. 474 pp.

Prezzi, C., Alonso, R., 2002. New Paleomagnetic data from the Northern Argentine Puna: Central Andes Rotation Pattern Reanalysed. J. Geophys. Res. 107 (B2), doi: 10.1029/2001JB000225.

Randall, D., 1998. A new Jurassic-Recent apparent polar wander path for South America and a review of central Andean tectonic models. Tectonophysics 299, 49–74.

Roperch, P., Fornari, M., Hérail, G., Parraguez, G., 2000. Tectonic rotations within the Bolivian Altiplano: implications fot the geodynamic evolution of the central Andes during the Late Tertiary. J. Geophys. Res. 105, 795–820.

Rousse, S., Gilder, S., Farber, D., McNulty, B., Patriat, P., Torres, V., Sempere, T., 2003. Paleomagnetic tracking of mountain building in the Peruvian Andes since 10 Ma. Tectonics 22 (5), doi: 10.1029/2003TC001508.

Seggiaro, R., Aniel, B., 1989. Los Ciclos Volcánicos Cenozoicos del Area Coranzulí-Tiomayo, Jujuy, Argentina. Revista de la Asociación Geológica Argentina 44, 394–401.

Somoza, R., Tomlinson, A., 2002. Paleomagnetism in the Precordillera of northern Chile (22°30′S): implications for the history of tectonic rotations in the Central Andes. Earth Planet. Sci. Lett. 194 (3–4), 369–381.

Somoza, R., Singer, S., Coira, B., 1996. Paleomagnetism of upper Miocene ignimbrites at the Puna, an analysis of vertical-axis rotations in the Central Andes. J. Geophys. Res. 101, 11387–11400.

Somoza, R., Singer, S., Tomlinson, A., 1999. Paleomagnetic study of upper Miocene rocks from northern Chile: implications for the origin of late Miocene-Recent tectonic rotations in the southern central Andes. J. Geophys. Res. 104, 22923–22936.

Torsvik, T., 1992. IAPD interactive analysis of paleomagnetic data, 51 pp. Geological Survey Norway, Trondheim.

Zijderveld, J.A.A., 1967. AC demagnetization of rocks: Analysis of results. In: Collinson, D.W., Creer, K.M., Runcorn, S.K (Eds.), Methods in paleomagnetism. Elsevier, Amsterdam, pp. 254–286.